Construction of Small-Diameter Vascular Graft by Shape-Memory and Self-Rolling Bacterial Cellulose Membrane

Ying Li, Kai Jiang, Jian Feng, Jinzhe Liu, Rong Huang, Zhaojun Chen, Junchuan Yang, Zhaohe Dai, Yong Chen, Nuoxin Wang, Wenjin Zhang, Wenfu Zheng, Guang Yang,* and Xingyu Jiang**

Bacterial cellulose (BC) membranes with shape-memory properties allow the rapid preparation of artificial small-diameter blood vessels when combined with microfluidics-based patterning with multiple types of cells. Lyophilization of a wet multilayered rolled BC tube endows it with memory to recover its tubular shape after unrolling. The unrolling of the BC tube yields a flat membrane, and subsequent patterning with endothelial cells, smooth muscle cells, and fibroblast cells is carried out by microfluidics. The cell-laden BC membrane is then rerolled into a multilayered tube. The different cells constituting multiple layers on the tubular wall can imitate blood vessels in vitro. The BC tubes (2 mm) without cell modification, when implanted into the carotid artery of a rabbit, maintain thrombus-free patency 21 d after implantation. This study provides a novel strategy for the rapid construction of multilayered small-diameter BC tubes which may be further developed for potential applications as artificial blood vessels.

1. Introduction

This study describes a method for the rapid preparation of artificial small-diameter vascular structures by employing bacterial cellulose (BC) membranes with self-rolling and tubular shape-memory properties. Cardiovascular diseases constitute a leading cause of mortality worldwide.[1] Cardiovascular regenerative medicine has emerged as a promising approach to replace or regenerate damaged or diseased cardiovascular tissues.[2] Tissue engineering has potential for the in vitro development of autologous or allogeneic transplantable vascular conduits. The scaffold material used for tissue-engineered vascular graft creation should be biodegradable and nonimmunogenic, and it must possess a high porosity and a microstructure that favor cell adhesion.[3] The replacement of lesion sites with an autologous vein is one of the most effective treatments available to date. However, the supply of usable veins in an individual is very limited. The rapid development of artificial blood vessels potentially provides an alternative way to address this problem.[4] The artificial vessels commonly used in clinical trials are currently made from synthetic materials such as expanded polytetrafluoroethylene, poly(ethylene terephthalate) (PET), and poly(glycolic acid).[4–7] While successful for large diameter (>5 mm) high-flow vessels, these synthetic materials are compromised by both thrombogenicity and compliance mismatch in low-flow for small-diameter blood vessels.[8–10] Shape-memory polymers (SMPs), proposed as biomaterials for minimally invasive surgical devices, have gained increased attention over the last several years.[11–14] Heat, light, or the local chemical environment

Dr. Y. Li, R. Huang, J. C. Yang, Z. H. Dai, N. X. Wang, Prof. W. F. Zheng, Prof. X. Y. Jiang
CAS Center of Excellence for Nanoscience
Beijing Engineering Research Center for BioNanotechnology
for Biological Effects of Nanomaterials and Nanosafety
National Center for NanoScience and Technology
Beijing 100190, China
E-mail: zhengwf@nanoctr.cn; xingyujiang@nanoctr.cn

Prof. X. Y. Jiang
University of Chinese Academy of Sciences
Beijing 100049, China

Dr. Y. Li, J. C. Yang, Prof. G. Yang
National Engineering Research Center for Nano-Medicine
Department of Biomedical Engineering
College of Life Science and Technology
Huazhong University of Science and Technology
Wuhan 430074, China
E-mail: yangsunny@yahoo.com

Prof. K. Jiang, Dr. J. Feng, J. Z. Liu, W. J. Zhang
Institute and Hospital of Hepatobiliary Surgery
Key Laboratory of Digital Hepatobiliary
Surgery of Chinese PLA
Chinese PLA Medical School
Chinese PLA General Hospital
Beijing 100190, China

Prof. Z. J. Chen
College of Chemical Engineering
Qingdao University
Qingdao 266071, China

Prof. Y. Chen
Ecole Normale Supérieure
24 rue Lhomond, Paris 75231, France

DOI: 10.1002/adhm.201601343

can activate the shape memory processes.[15–17] Although SMPs have been used as stents in treating cardiovascular diseases, only a few investigations concern artificial blood vessels with shape-memory materials.[18] Besides SMPs, shape memory can also be achieved by materials without intrinsic shape-memory properties. In our previous work, multilayered tubes were obtained through the stress-induced rolling membrane (SIRM) technique, by preloading an inner stress in a polymer membrane (not shape memorable) which mimics the structure and functions of tubular tissues.[19–22] Our pioneering work paves an avenue for the rapid fabrication of shape-memory tubular structures using nonshape-memory materials.

BC is biosynthesized by *Gluconacetobacter xylinus* (*G. xylinus*) and can be used as scaffold for tissue engineering of cartilage, skin, dental, nerve, and blood vessels.[23–26] These applications benefit from its unique properties such as a high mechanical strength, high permeability, high water-holding capacity, good biocompatibility, and low toxicity.[27,28] BC implanted subcutaneously in rats for 1, 4, and 12 weeks neither showed macroscopic signs of inflammation around the implants nor demonstrated the presence of any fibrotic capsule or giant cells.[29] Commercial products of BC such as Biofill and Gengiflex are widely applied in surgery and dental implants.[24] BC cannot be degraded in the human body due to the absence of cellulases.[30,31] However, the non-biodegradability of BC provides it a high stability as an implantable material. Biosynthesized BC tubular structures with various diameters were recently used as artificial blood vessels in animals for long-term, thrombosis-free implantations.[32–34] In previous studies, the properties of single-layer tubular BC were characterized and demonstrated excellent performance as artificial blood vessels. The dynamic clotting time for biomaterials should be ideally above 40 min. A longer clotting time reflects high biocompatibility of the material. Similarly, a hemolysis rate of less than 1% indicates good biocompatibility for any biomaterial (corresponding to ISO 10993-10:1995). Our previous work showed that the in vitro dynamic clotting time of BC tube can exceed 60 min, while the hemolysis rate was evaluated to range from 0.097% to 0.42%, indicating excellent performance of BC as vascular implant.[35] However the in situ, one-step fabrication of BC tubes in previous studies faced several major problems including: (1) complex devices required for producing tubular BC, (2) uneven densities of BC fibers in different parts of the tube due to the variable supply of oxygen during BC biosynthesis, (3) longer culturing time required than for planar BC with the same volume, and (4) difficulty in producing multilayered tubes, which is essential for simulating the structure of real blood vessels. A recently reported method partially solved these problems. The blocks of BC were perforated with a metallic needle, dried, and freeze dried to form tubular structures which showed more than 1 month of patency in vivo as an artificial blood vessel.[36] However the one-layer tube still does not resemble native blood vessels, which are multilayered. One of the effective ways for solving this problem is to produce BC tubes based on planar BC membrane, which is simple, fast, and highly tunable. For instance, the thickness and size of a BC membrane can be adjusted by varying the bacterial culturing time and chamber size. Furthermore, the planar BC membrane could be rolled into a multilayered tube to simulate various tubular structures in the human body. Herein, we want to use the SIRM technique to transform planar BC membranes into tubular structures. One of the main requirements for SIRM is the elastic nature of at least one of the layers of the polymeric membrane. In our previous works, tubular structures were fabricated using nonelastic materials such as polycarbonate and PET, with the help of prestressed elastic polydimethylsiloxane (PDMS) strips.[20] Although the nonelastic BC membrane could be prepared to form a tube by a similar strategy, the removal of the strips before implantation sometimes leads to changes in the shape of the tube. Furthermore, longer tubes need more elastic strips in the middle part of the BC membrane, such that they could not be removed after the BC tube formation. To avoid the use of elastic strips, we hope to produce an inner stress in the BC membrane to maintain the shape of the BC tube.

In this study, a strategy to build stress (shape-memory) in the BC membrane for the rapid transformation of a 2D membrane into a 3D multilayered tubular structure is reported. Multilayered tubular BC structures were obtained by molding and lyophilizing treatment of BC membranes. Unrolling of the BC tube into a flat membrane by an external force allowed the precise patterning of human umbilical vein endothelial cells (HUVECs), human aortic smooth muscle cells (HASMC), and human skin fibroblasts (HSF) on its surface by microfluidics. The shape-memory property of the BC membrane allowed it to reroll into a multilayered tubular structure with properly patterned multiple types of cells, which mimics a natural blood vessel. As artificial blood vessels, the transplanted shape-memory BC tubes (without cell modification) in the carotid artery of rabbit maintained long-term patency (21 d of observation). Thus, by exploring and employing an intrinsic property of BC, we paved a new way for the rapid preparation of multilayered tubular structures with potential applications in vascular tissue engineering.

2. Results and Discussion

2.1. Preparation and Characterization of the BC Tube

A BC membrane was obtained by culturing *G. xylinus* using a multiple layers fermentation method.[37,38] After sterilization, purification, and appropriate shape trimming, the wet BC membrane was rolled onto a stainless steel mandrel (2 mm diameter) from one side to the other to form a multilayered tubular structure (**Figure 1**A) followed by lyophilization at −60 °C for 6 h. When the mandrel was removed, a free-standing multilayered BC tube was obtained. The morphological properties of the BC tube were determined by scanning electron microscopy (SEM). SEM micrographs of a cross-section of the BC tube showed a three-layered wall (Figure 1B,C). Magnified images showed that the BC layer was composed of interwoven nanofibers (Figure 1D). SigmaScan Pro 5.0 analysis indicated that the diameter of the fibers was about 115 nm and the size of the pores between the fibers was about 140 nm. The pores can be beneficial for the exchange of nutrients and waste between the layers. The macrographs of the lyophilized BC tube showed visible spaces between the layers (Figure 1E). The spaces became invisible after the BC tube was immersed in

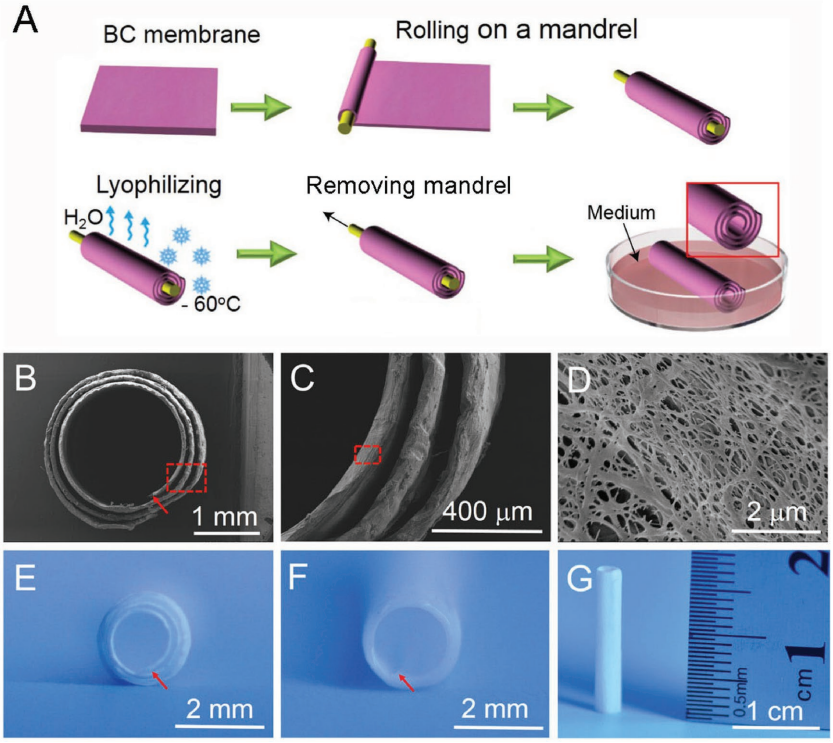

Figure 1. Preparation and characterization of a multiple cell-laden BC tube. A) Schematic illustration of the fabrication process of the BC tube. B) SEM image of a BC tube with three-layered walls. C) Magnified image of the tube in (B). D) Magnified image of the tube in (C). E) Photographs of a lyophilized BC tube. F) Photograph of the same BC tube in (E) in the wet state. G) Photograph of the same wet tube in (E). The tube can stand on a flat surface. Red dashed rectangles in (B) and (C) show the magnified zones. Red arrows in (E) and (F) indicate the interlayer interface of the tube.

water for 30 min, before the excess water was removed by pressing with a steel mandrel (Figure 1F). These observations indicate that multiple layers of BC tube could "merge" together to form an integrated wall for the vessel, if it is grafted in the human body as a section of blood vessel in an environment with blood and interstitial fluids.

Mechanical properties are pivotal in determining the performance of cardiovascular grafts.[10] One of the essential requirements for a BC tube to serve as a vessel in the human body is mechanical strength sufficient for microsurgery. Moreover, the BC tube must not only resist mechanical strain in microsurgical preparation and anastomosis but also be able to withstand the blood pressure.[33,39] The wet BC tube can stand by itself (Figure 1G), demonstrating that it can support its own weight. The mechanical properties of the BC tube were tested with a universal mechanical analyzer, using a rabbit carotid artery as a control. The ductility of the rabbit carotid artery and the BC tube was about 0.22 and 5.93 J m^{-2}, respectively. Similarly, the strength of the rabbit carotid artery and tubular BC was about 0.19 and 61.9 MPa, respectively. Thus, the ductility and strength of tubular BC are much better than for the rabbit carotid artery. These results, combined with previous studies that demonstrated the superior mechanical properties of BC over the majority of synthetic materials in shape retention and tear resistance, led us to believe that BC tubes were strong enough for vascular implantation.[40]

To explore the shape-memory property of the BC tube, lyophilization-treated tubular BC (BC-t) and tubular BC without lyophilization treatment (BC-n) were prepared to verify whether lyophilization is a key process in the generation of shape memory. Tubular weighing paper (W) and filter paper (F) were also subjected to the same production procedures as the lyophilization-treated BC tube to serve as controls (**Figure 2**A). The four kinds of tubes were soaked in DMEM medium for 30 min (Figure 2B), followed by unrolling on a flat surface and drying at room temperature to maintain their flat-shaped state (Figure 2C). The flat samples were then resoaked in the Dulbecco's Modified Eagle's medium (DMEM) and allowed to reroll into tubes (Movie S1, Supporting Information). The rerolled BC tube showed tight packing of the multiple layers. The inner diameter

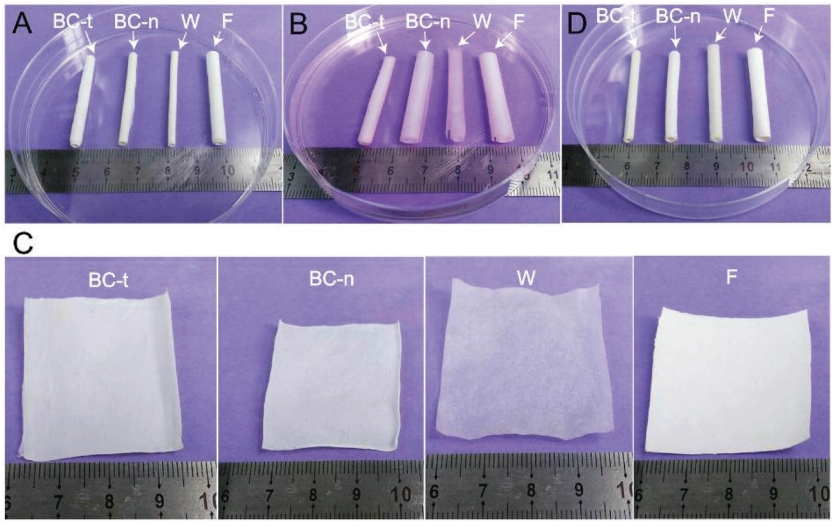

Figure 2. Optical images of lyophilization-treated tubular BC (BC-t), nonlyophilization-treated tubular BC (BC-n), lyophilization-treated weighing paper (W), and lyophilization-treated filter paper (F) at different states. A) Newly prepared tubes of the different materials. B) Appearance of the different tubes after soaking in DMEM medium for 30 min. C) After soaking in DMEM medium for 30 min, the tubes were unrolled on a flat surface at room temperature until they became dry. D) The rerolled tubes.

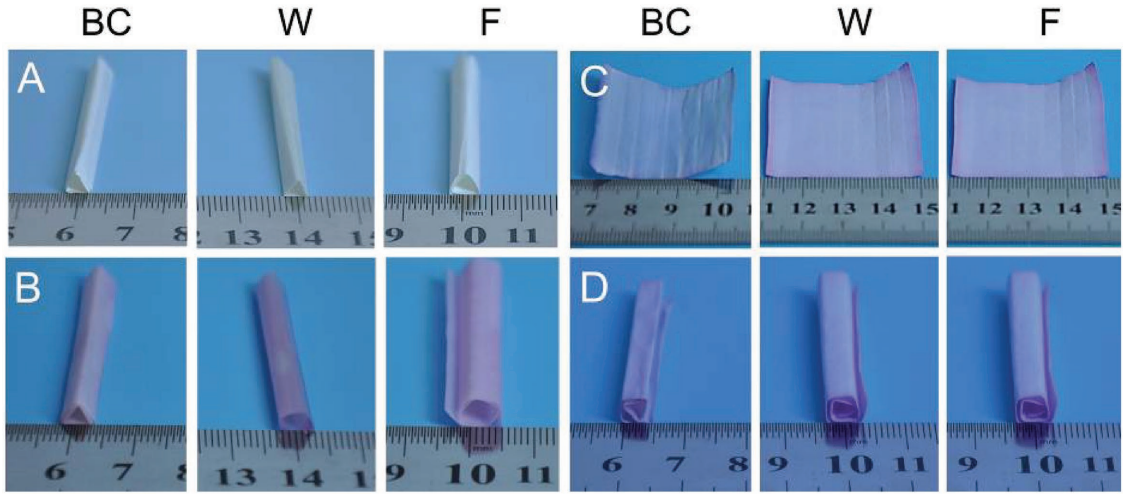

Figure 3. Optical images of triangle-shaped BC (BC), weighing paper (W), and filter paper (F) at different conditions. A) Lyophilized triangle-shaped BC, weighing paper, and filter paper. B) Triangle-shaped BC, weighing paper, and filter paper soaked in DMEM medium for 30 min. C) Triangle-shaped BC, weighing paper, and filter paper unrolled and dried in air. D) Rerolled triangle-shaped BC, weighing paper, and filter paper.

of the BC tubes in the original and rerolled states was essentially identical (Figure 2D). In contrast, the rerolled BC tube without lyophilization treatment, weighing paper tube, and filter paper tube were loosely packed with increased inner and outer diameters (Figure 2D). Thus the lyophilization-treated BC tube showed excellent performance in terms of memory of its original shape. To confirm the shape-memory property of the lyophilization-treated BC membrane, the same method was used to prepare tubes with various cross-sectional shapes (**Figure 3**). Tubular BC, filter paper, and weighing paper with a triangle-shaped cross-section were fabricated (Figure 3A). After the medium soaking (Figure 3B), unrolling (Figure 3C), and rerolling (Figure 3D) processes, the deformation of the BC tube was lowest among the three types of materials. Screw-shaped BC was also prepared and demonstrated excellent ability in maintaining its original shape after immersion in phosphate buffer saline (PBS) solution for 3 months or longer time periods (Figure S1A,B, Supporting Information). The micromorphology of the outer and inner sides (Figure S1C,D, Supporting Information) of the screw-shaped BC tube was characterized by SEM. There were several parallel cracks in the inner side of the BC tube, which were produced by pressing of the BC membrane on the parallel bulges of the screw-shaped mandrel during the fabrication process (Figure S1E, Supporting Information). When scanning the areas around the cracks, the BC fibrils displayed a tendency for parallel arrangement along the direction of the cracks (Figure S1F–H, Supporting Information).

The shape-memory mechanism of the BC tubes was also studied. The BC fibers may experience rearrangements during molding on the mandrel and the lyophilization procedure, which may contribute to the shape memory of the BC tubes. To verify this hypothesis, the SEM characterization of BC membranes before and after molding and lyophilization treatments was carried out. As demonstrated in our previous study, the size and density of fibers at the top and bottom sides of the BC membrane are different due to the different oxygen supply on the two sides during the biosynthesis process by bacteria.[38] The top side of the BC membrane had more compact and denser fibrils than the bottom side.[38] The size of the fibers and pores was analyzed by SigmaScan Pro 5.0, by randomly selecting three replicate samples and measuring 40 fibers or pores on each sample ($n = 120$). The diameter of the fibers was 292 ± 215 and 188 ± 104 nm on the top and bottom sides of the BC membrane, respectively. Similarly, the size of the pores on the top and bottom sides of the membrane was 168 ± 93 and 320 ± 198 nm, respectively (**Figure 4**A_3,B_3 and Figure S2 (Supporting Information)). The fibrils on each side were all randomly arranged (Figure 4A–A_3,B–B_3). During fabrication of the BC tube, the top and bottom sides of the BC membrane were rolled and formed the inner and outer sides of the layers on the tube, respectively (Figure 4C–C_3,D–D_3). There were many parallel creases on the surface of the inner and outer sides of the BC tube, whose directions were perpendicular to the rolling direction (Figure 4C–C_3,D–D_3). These creases may be produced during the rolling processes and fixed by the lyophilization process. The creases on the inner side were more prominent than their counterparts on the outer side. The connectivity of the fibers at the crease sites was poorer as compared to other locations. There were also more pores at the crease sites than at other places (Figure 4C_2,D_2). The magnified images indicate that the BC fibers were more ordered at the crease sites. Thus, the creases on the BC layers and the specific arrangement of the fibers at the crease areas should generate an inner stress on the layers and drive the self-rolling of the BC tubes.

Besides the arrangement of the fibers on the BC tube, their size and density were also characterized by the same method used for the BC membrane. The diameter of the fibers was about 77 ± 44 and 61 ± 40 nm on the rolled BC-inside-top (R-BC-I-T) surface and rolled BC-outside-bottom (R-BC-O-B) surface of the BC tube, respectively. Similarly, the size of the pores on the R-BC-I-T side and R-BC-O-B side of the BC tube was about 590 ± 559 and 404 ± 209 nm, respectively (Figure 4C_3,D_3 and

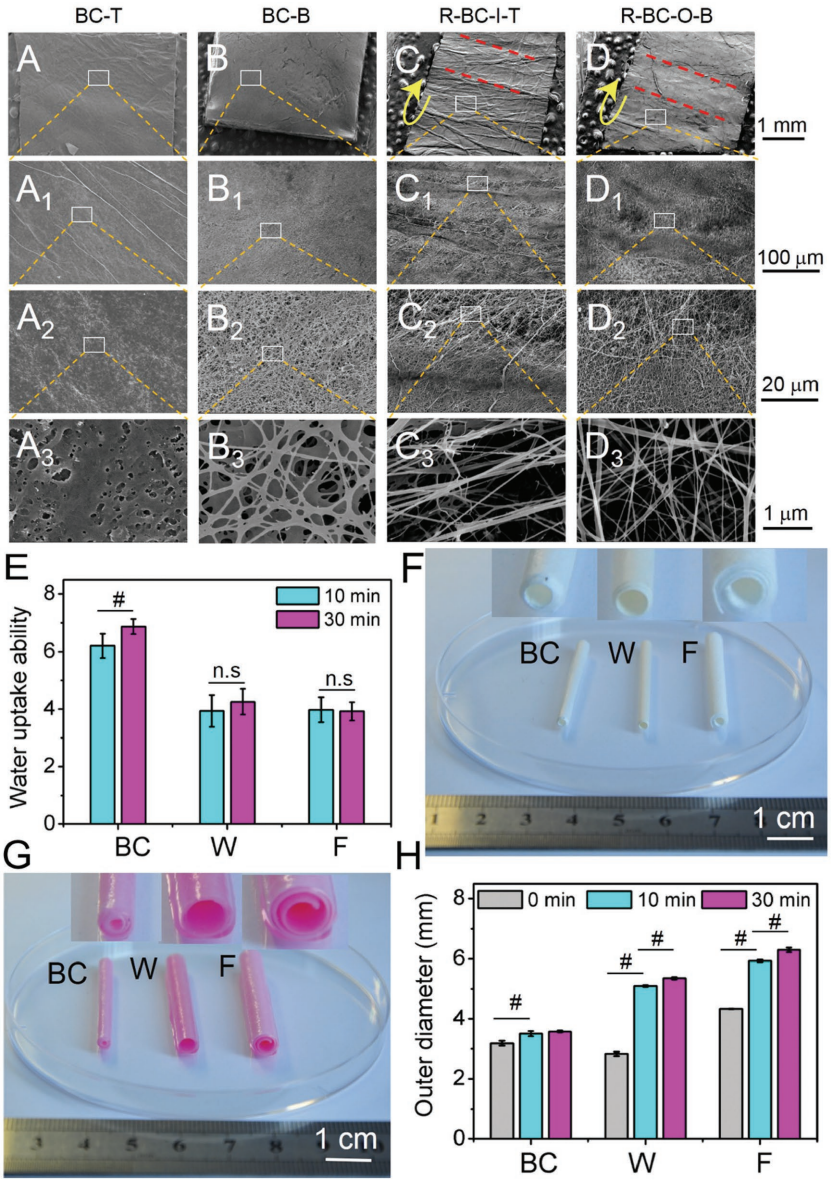

Figure 4. Characterization of tubular BC, weighing paper, and filter paper. A–D) SEM images of the BC-top surface (BC-T), BC-bottom surface (BC-B), rolled BC-inside-top surface (R-BC-I-T), and rolled BC-outside-bottom surface (R-BC-O-B). The white rectangles indicate the magnified parts of the images. The red dashed lines represent creases on the BC membrane. The yellow arrows indicate the rolling direction of the membrane. E) Water uptake ability of BC membrane, weighing paper, and filter paper. F) Photograph of dry tubes of BC (BC), weighing paper (W), and filter paper (F) on a dish. G) Macroscopic view of wet tubes of BC (BC), weighing paper (W), and filter paper (F) on a dish. The tubes were immersed in DMEM medium for 30 min before imaging. H) Variation in the diameter of tubular BC (BC), weighing paper (W), and filter paper (F) before and after immersion in DMEM medium for 0, 10, and 30 min ($n = 6$, $^{\#}P < 0.01$, the standard error means standard deviation (SD)).

Figure S2 (Supporting Information)). As compared to the flat BC membrane, tubular BC showed thinner fibers and larger pores, which could facilitate the infiltration of macromolecules and improve the biocompatibility of the BC tubes.

The water uptake capacity of the BC membranes was also assessed, since it may influence its thickness and mechanical strength after implantation. Weighing paper and filter paper were used as controls. The BC membrane, weighing paper, and filter paper were cut into flat squares of the same size (2×2 cm^2). After immersion in PBS solution for 10 min, the weight of the tubular BC, weighing paper, and filter paper samples was found to be 6.2, 3.9, and 4.0 times their initial weight, respectively (Figure 4E). When the incubation time was extended to 30 min, the water uptake by tubular BC and weighing paper was about 6.9 and 4.2 times the original weight, respectively, while the filter paper showed a negligible change (Figure 4E). There were significant differences among the three groups ($P < 0.01$, analysis of variance, ANOVA), and the BC membrane had the best water uptake capability. The different water uptake capabilities of the three materials are attributed to their different nano- or microstructure. The BC membrane had thinner fibers and more nanopores than both the weighing paper and filter paper (Figure S3, Supporting Information). These observations demonstrate that BC tubes possess more space for water preservation. The variation in their shape was compared before and after immersion in DMEM medium (30 min). All three tube types were white in color and possessed the same inner diameter before immersion in the medium (≈2.0 mm, Figure 4F). Due to the different thickness and mechanical properties of the three materials, the outer diameter of the tubes was different (BC ≈3.2 mm, W ≈2.8 mm, F ≈4.3 mm, Figure 4H). When the tubes were immersed in the medium for 10 min, all changed to a pink color due to the adsorption of dyes in the medium (Figure 4G). The BC tube maintained the same shape as the preimmersion state and displayed size variations with an inner diameter of ≈1.5 mm and an outer diameter of ≈3.5 mm (Figure 4G). The diameter of the weighing paper and filter paper tubes significantly increased as compared to their dry counterparts (W, inner diameter ≈2.3 mm, $P < 0.01$, t-test; outer diameter ≈5.0 mm, $P < 0.01$, t-test; F, inner diameter ≈3.2 mm, $P < 0.01$, t-test; outer diameter ≈5.9 mm, $P < 0.01$, t-test; Figure 4H). When the incubation time was increased to 30 min the outer diameter of the BC tube increased to 3.6 mm, which is an insignificant variation as compared to its size at 10 min (t-test, $P > 0.05$). In contrast, the tubes made with weighing paper and filter paper displayed a significant size increase as compared with their size at 10 min (W: t-test, $P < 0.01$; F: t-test, $P < 0.01$; Figure 4H). These results demonstrate the superiority of the BC tubes over the weighing paper and filter paper tubes in maintaining their shape in DMEM medium.

2.2. In Vitro Evaluation of the Cell-Laden BC Tube

The BC tube was unrolled with tweezers and fixed onto the surface of a Petri dish, by placing a small amount of culture medium between the BC membrane and the surface, to fabricate the cell-laden tube. Different types of cells were patterned on the BC membrane by the microfluidic chip technique, to simulate a real blood vessel in vitro. Typical artery vessels consist of three layers arranged in a concentric manner: intima, media, and adventitia. In this study we patterned HUVECs, HASMC, and HSF to the specific areas of the unrolled BC membrane and let the BC membrane reroll automatically to form a three-layered, cell-laden tube to simulate a blood vessel.[41] A microfluidic chip made of PDMS and a microdevice containing three parallel channels was placed onto the flat BC membrane. By introducing different cell types through the different microchannels, the cells were patterned onto the BC membrane at specific positions after 24 h of culture at 37 °C and 5% CO_2. After peeling off the microfluidic chip, the flat BC membrane with patterned cells rerolled into a multilayered cell-laden tube in the culture medium automatically (**Figure 5**A). The cell-laden BC tube could be incubated in the medium for a longer time (>10 d) to allow proliferation of the cells and the secretion of extracellular matrix by the cells.

The cultured cells on the BC tubes were characterized by staining different types of cells with different dyes (blue: HUVECs, green: HASMC, and red: HSF) before their delivery onto the unrolled BC membrane with the microfluidic chip. After the cells attached onto the tubular BC membrane (before rolling) for 24 h, these were observed by confocal microscopy. The three types of cells confined to specific regions of the unrolled membrane can form different layers of cells on the vessel after rolling. Each type of cell was evenly distributed under a large visible field (Figure 5B(a)). Magnified images randomly selected from regions corresponding to each type of cell showed that the cells had normal morphologies (Figure 5B(b)). Once the cells on the BC membrane grew and formed a confluent monolayer, the cell-laden membrane was allowed to roll-up and transform into a tube through its internal stress. Cross-sectional images showed the differently stained cells from the inside to the outside: HUVECs (blue), HASMC (green), and HSF (red) (Figure 5B(c)), resembling the structure of a natural human blood vessel. We further characterized the morphology of the three types of cells cultured on the BC tube for 1 and 3 d, respectively, via SEM (Figure 5C). The BC tube was unrolled before imaging. Each cell type firmly attached to the membrane by extending fillopodia or spreading lamillipodia on day 1. With increasing culture time, each cell type grew and covered the entire surface of the membrane, which indicates that the tubular BC membrane facilitated rapid proliferation of the cells.

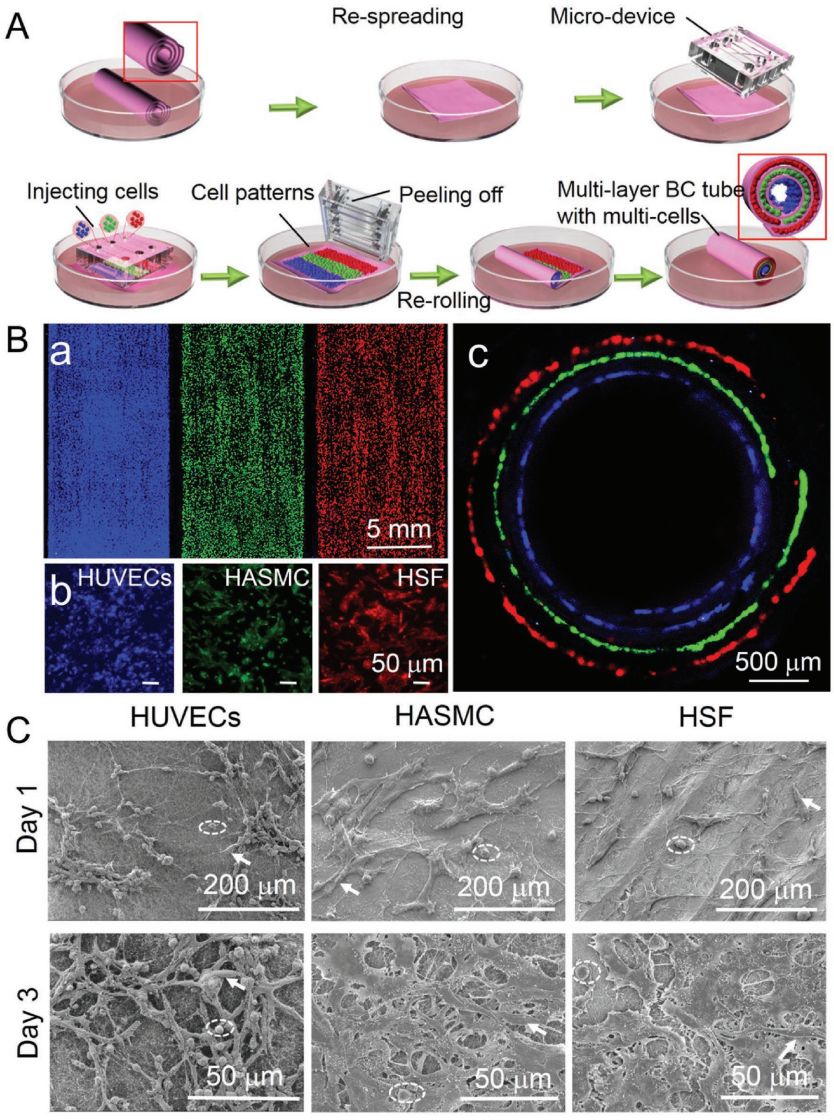

Figure 5. Patterning and culture of HUVECs, HASMC, and HSF cells on BC tubes to mimic a natural blood vessel. A) Schematic representation of the patterning of three cell types on a 2D BC membrane and rolling of the BC membrane into a multilayered cell-laden tube in vitro. B) Three cell types on BC membrane before (a, b) and after rolling (c). The blue, green, and red fluorescence indicates HUVECs, HASMC, and HSF, respectively. The magnified images in (b) were randomly selected from the regions of each type of cell in (a). C) SEM images show the morphology of HUVECs, HASMC, and HSF attached to the BC tube on day 1 and day 3. Spindle-shaped cells are represented by an arrow, while round-shaped cells are shown by a dashed ellipse.

We further characterized the cell compatibility of the BC membranes by seeding HUVECs, HASMC, and HSF on the BC membranes and culturing them in DMEM medium containing 10% fetal bovine serum (FBS) at 37 °C and 5% CO_2 for different time periods. Calcein acetoxymethyl ester (Calcein

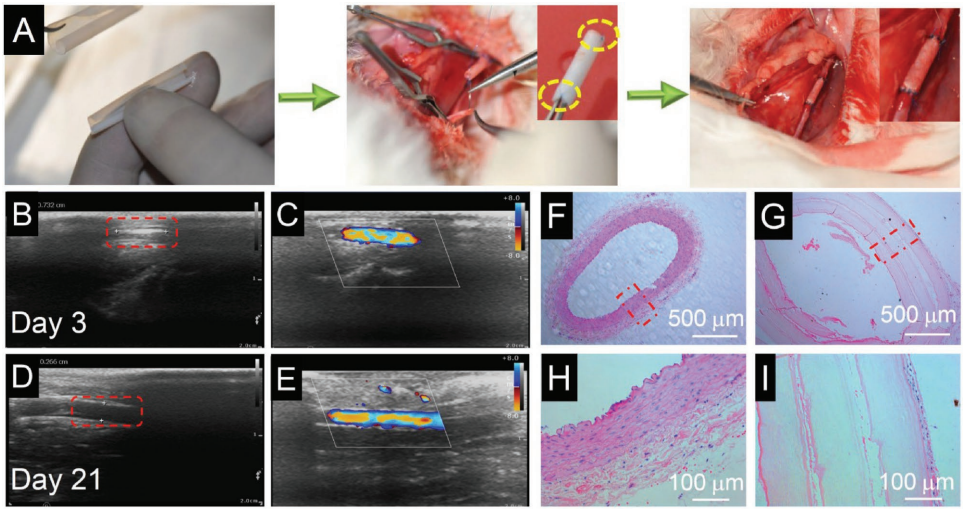

Figure 6. Evaluation of the BC tube in rabbits. A) Photographs showing the implantation process of the BC tube. Ultrasound images (B,D: B-mode; C,E: color Doppler blood flow imaging) of the BC tube implantation on the carotid artery of rabbits on B,C) day 3 and D,E) day 21 postoperation. The transplanted BC tube had high flow without signs of restenosis or aneurysm. Microscopic images of F,H) HE staining of the cross-sections of normal rabbit carotid artery and G,I) the BC tube transplanted on the carotid artery of rabbits after three weeks. (H) and (I) are magnified parts of (F) and (G) marked with dashed red rectangles, respectively.

AM)-green staining demonstrated that the cells maintained a high level of viability (Figure S4A,B, Supporting Information). The CCK-8 assay further confirmed rapid proliferation of the three cell kinds (Figure S4C, Supporting Information). We also evaluated the extracellular medium secretion of the cells on the BC membrane. Specific immunological staining demonstrated that cells cultured for 5 d secreted Collagen I, which attached to the BC fibers around the cells (Figure S5, Supporting Information). These results denote the good cell compatibility of the BC membrane.

2.3. In Vivo Analysis of the Cell-Free BC Tube

The performance of tubular BC was further evaluated in vivo, by implanting it in a rabbit to replace a segment of the carotid artery with a diameter of ≈0.195 cm (**Figure 6**A and Figure S6 (Supporting Information)). The dynamic blood flow of the implanted BC tube was observed by Doppler ultrasound imaging (Philips ultrasound, CX Cart). Two modes of ultrasound images were used in this study: B-mode ultrasound (Figure 6B,D) and color Doppler blood flow imaging (Figure 6C,E). B-mode ultrasound imaging gave the echo signal, while color Doppler blood flow imaging provided the blood flow signal. The B-mode images show that the BC tube connected to the proximal and distal ends of the carotid artery exhibited high echo signals (bright) 3 d postoperation (Figure 6B). The length and diameter of the transplanted BC tube was about 0.71 and 0.23 cm, respectively, similar to their size before implantation (i.e., length, 0.73 cm, diameter, 0.25 cm) (Figure 6B). Doppler ultrasound imaging at the third day postoperation showed that there was a strong blood flow signal through the transplanted BC tube during the systole of the cardiac cycle (Figure 6C). After implantation for 21 d, B-mode ultrasound imaging showed that the echo signal of the implanted BC tube became weaker as compared with that on day 3 (Figure 6D), which may be attributed to encapsulation of the BC tube by host tissues in the vicinity. The boundary between the implanted BC tube and the host carotid artery became invisible on the ultrasound images, and therefore the length of the BC tube could not be measured. The diameter of the implanted BC tube was about 0.266 cm (Figure 6C), which was slightly larger than on day 3. This is ascribed to remodeling of the BC tube, due to a balance between mechanics from the blood pressure, blood flow, and surrounding tissues. The inner side of the BC tube was relatively straight and smooth, without any visible thrombus. Doppler ultrasound observations indicated apparent blood flow signals throughout the implanted BC tube 21 d postimplantation (Figure 6E).

The performance of the implanted BC tube in the rabbit carotid artery for 21 d was further verified by hematoxylin–eosin (HE) staining of the dissected tissues. The implanted BC tube had a round-shaped cross-section and smooth inner layers (Figure 6G). There were neither thrombus nor immune cells present on the inner side of the BC tube, which demonstrates the excellent biocompatibility of the BC material and ideal mechanical properties of the multilayered BC tube (Figure 6G). The multiple layers of the BC tube could "merge" together after removal from the medium (Figure 1F), and the two ends of the tubular BC were sutured to maintain tight packing of the different layers before implantation. The BC layers remained packed without large spaces nor immune cells between them after implantation (Figure 6I). We speculate that the BC layers of the tube must be tightly packed in vivo, since otherwise the blood components would enter into the interspace of the layers, and either provoke an immune response (immune cells such as monocytes or leukocytes) or induce thrombus formation. The outer layer of the BC tube, having smooth interfaces with the host tissues, showed ingrowth of the host cells (Figure 6I), which demonstrates that although BC is not biodegradable, it

allows fusion with the host tissues, facilitating remodeling of the implanted tubes responding to the microenvironment of the blood vessel. As compared with the natural carotid artery (Figure 6F,H), having an elliptical cross-section with integrated multiple cellular layers and a clear lumen, the BC tube showed a similar configuration and antithrombosis properties (Figure 6G). To prevent thrombosis postimplantation, the BC tube was immersed in heparin-NaCl solution (low molecular heparin sodium) for 10 min before implantation, and injected with heparin-NaCl solution every day, 5 d postimplantation. Thus, the BC tube has the potential to serve as artificial blood vessel for vascular tissue engineering. A previous study showed that thrombus and graft occlusion appeared within one week for implanted two-layer poly (DL-lactide-co-glycolide) (PLGA) tubes (5 mm in diameter), and that the attachment of endothelial cells inside the PLGA tube could prolong the nonthrombosis state to three weeks.[42] In the current study, even the BC tube without cell modification displayed excellent patency in vivo for over 21 d, which is comparable to the performance in a recent report on one-layer cell-free BC tubes.[36] Furthermore, the inner diameter of the BC tube in the current study was only about 2 mm, which is smaller than the recently reported BC tube and matches the size of typical small-diameter blood vessels such as coronary arteries in the human body.[36] Thus, tubular BC appears to be a promising candidate to be used for small-diameter vascular grafts.

We did not use cell-laden BC tubes in the in vivo experiments in this study, considering the possible incompatibility of the host–guest cells. Increasing evidence indicates the excellent performance (very low inflammatory and immunological reactions) of BC in vivo.[29,36] Thus, in situ tissue engineering based on BC may be a perfect solution for the translation of this approach to the clinic. Specific growth factors or transcription factors could be patterned in specific areas of a piece of 2D BC membrane, such that when the 2D BC self-rolls into a 3D vessel and is implanted into the body, the growth or transcription factors in different layers of the vessel induce the ingrowth and differentiation of host progenitor cells to form cell layers mimicking real blood vessels. The tedious work including cell source seeking, cell separation and purification from donors, and cell patterning could be simplified by in situ patterning of the growth factors or transcription factors. Furthermore the issues of immunological reactions, inflammation and contamination, and cell viability could be avoided. We think that in situ tissue engineering is a truly practical method for the translation of our approach.

3. Conclusions

In summary, we report a strategy to rapidly fabricate multilayered artificial blood vessels by employing the shape-memory property of BC membranes. The creases on the membrane, as a result of the rearrangement of the BC nanofibers, are believed to be responsible for the shape-memory of the material. After cell attachment in a flat state, the BC membrane can return to its original shape as multilayered tubular structures, to serve as small-diameter artificial blood vessels. The excellent shape-maintaining performance of the BC tube in vitro and in vivo demonstrates its reliability as a vascular graft. Active proliferation of the cells in the BC tube in vitro and the long-term (21 d) thrombosis-free performance of the (cell free) BC tube in vivo demonstrate the success of our strategy in exploring and utilizing a new property of the BC material and may be promising for small-diameter blood vessel tissue engineering and other vessel-like structures.

4. Experimental Section

Preparation of the BC Membrane: *G. xylinus* (ATCC58532, American Type Culture Collection, USA) was cultured on Hestrin and Schramm (HS) medium. The HS medium was sterilized for 20 min at 121 °C and inoculated with the bacteria in an Erlenmeyer flask (10%, v/v). The multiple layers fermentation method was used to obtain multiple layers and homogeneous BC membranes.[37] After two weeks, the BC membrane was harvested and treated with Milli-Q water and 1 wt% NaOH until pH 7.0 was obtained. The BC membrane was then sterilized and stored at room temperature for future use.[38]

Preparation of Tubular BC, Weighing Paper, and Filter Paper: Sterilized wet BC membrane, weighing paper, and filter paper were immersed in Petri dishes containing cell culture medium. After 30 min, all the samples were harvested and placed onto a piece of flat and dry glass. About 80%–90% of the water was squeezed from the wet BC membrane. The wet BC membrane, weighing paper, and filter paper were cut into squares (4×4 cm^2) and rolled onto a stainless steel mandrel (2 mm diameter and 6 cm length) from one side to the other to obtain multilayered tubular BC, weighing paper, and filter paper.[43] The mandrels were removed and the tubular BC, weighing paper, and filter paper were stored at −35 °C for 24 h followed by lyophilization at −60 °C for 6 h.

Morphology Characterization: The morphology of the BC membrane, weighing paper, and filter paper tubes was recorded using a Nikon camera (N16184, Japan), field emission scanning electron microscope (S4800, Hitachi), and confocal laser scanning microscope (CLSM) (LSM710, Carl Zeiss).

Water Uptake Ability: The BC membrane, weighing paper, and filter paper were cut into squares with a side length of 2 cm and immersed in PBS solution for various time intervals (10, 30 min, 1, 2, and 12 h) at room temperature. The samples were shaken twice to remove unbound water before weighing. The water uptake ability was calculated using the following equation as reported in a previous study[44]

$$W = (W_t - W_0)/W_0 \quad (1)$$

where W_t is the wet weight at different times and W_0 is the weight of the dry material.

Mechanical Strength Measurement: The tensile strength of the rabbit carotid artery and tubular BC (three layers) was measured on a universal mechanical analyzer (BTC-EXMULTI-PAC2). The samples were tested at a stretching speed of 5 mm min^{-1}.

Cell Culture and Staining: HUVECs, HASMC, and HSF were incubated in DMEM medium containing 10% FBS, 1% penicillin G (P) (100 U mL^{-1}), and streptomycin (S) (100 U mL^{-1}) (Invitrogen, USA). The cell culture medium was changed every 3 d and all the cells were cultured at 37 °C and 5% CO_2 in a humidified atmosphere. A 0.25% trypsin-0.53 $\times$ 10^{-3} M ethylenediaminetetraacetic acid (EDTA) solution was used to prepare the cell suspensions. All the cells were obtained from the bank of Peking Union Medical College (China). Three types of cells were patterned at specific positions of the tubular BC, to mimic structures found in natural blood vessels. The sterilized tubular BC was put in a Petri dish containing cell culture medium, tweezers were used to unroll it on the substrate, and a microfluidic chip was installed on the surface of the spread tubular BC. The dimensions of the microfluidic chip were about 5 mm in height, 4 cm in length, and 4 cm in width (one channel was about 1 cm $\times$ 3 cm). The cells were stained with different

dyes when they reached about 90% of confluence on the Petri dish, cell suspensions were prepared with a cell density of 1×10^7 cells mL^{-1}, and the cells were delivered on the flat BC membrane via each channel (500 µL). Cell tracker C34565, C3099, and C34551 were used to stain HUVECs, HASMC, and HSF, respectively. The microfluidic channels were peeled off after attachment of the cells on the BC membrane. The cells were washed twice with PBS and fixed with 4% paraformaldehyde (PFA) for 1–2 h at 4 °C. The PFA solution was removed and the cells were washed twice with PBS. The BC membrane containing the cells gradually rolled into a multilayered tube through its internal stress.

Calcein AM Staining: HUVECs, HASMC, and HSF cells were cultured after spreading on tubular BC (5×10^4 cells mL^{-1}) by the microfluidic chip method (5 mm height, 4 cm length, and 1 cm width) for 1, 3, and 5 d. The culture medium was then removed and PBS was used to wash the cells three times, and Calcein AM reagents (working concentration: 200×10^{-9} M, 1 mL) (Dojindo, Japan) were added before incubation for 20 min at 37 °C in 5% CO_2. A CLSM (LSM710, Carl Zeiss) was used to record fluorescence images after washing with PBS three times. Eight fields were randomly selected and the number of cells attached on the surface in a defined area was determined when the cells were observed at 100× magnification.

Cell Viability Assay: HUVECs, HASMC, and HSF cells were cultured on spread tubular BC (96-well plates) (1×10^4 cells, 200 μL^{-1}) for 1, 3, and 5 d, respectively. The culture medium was then removed, 200 µL of medium containing Cell Counting Kit (CCK-8) (20 µL) was added into each well, and the samples were incubated for 1 h. The medium was removed (100 µL) to another well before measuring the optical density of the samples on a microplate reader (Tecan, infinite M200, Switzerland) at 450 nm. The results were analyzed with Origin Pro 8.0.

Immunofluorescence Assay: HUVECs, HASMC, and HSF cells were cultured on spread tubular BC (5×10^4 cells mL^{-1}) by the channel microfluidic chip method for 5 d. The medium was removed before staining with Calcein AM assay reagents (200×10^{-9} M) for 20 min at 37 °C, and the cells were fixed with 4% PFA for 15 min at 4 °C before washing three times with PBS. Permeabilization buffer (0.5% Triton X-100 in water) was added and incubated for 15 min at 4 °C before washing with 1% bull serum albumin (BSA)/PBS for 30 min at 37 °C. The BSA/PBS was then removed and the cell-laden BC membrane was incubated in rabbit polyclonal to Collagen I (ab34710) (100 µg mL^{-1}, dilution 1:200 in 1% BSA/PBS solution) solution overnight at 4 °C. The medium was removed before washing three times with PBS. The secondary goat anti-rabbit lgG Alexa Fluor 555 (Invitrogen) (dilution 1:200 in 1% BSA/PBS solution) was added and incubated for 30 min at room temperature, and the samples were washed three times with PBS before the cells were observed at 100× magnification on a CLSM (LSM710, Carl Zeiss).

Animal Surgery and Histological Analysis: Male rabbits (Beijing Vital River Laboratory Animal Technology Co. Ltd., China) with an average weight of 3 kg were used in the in vivo experiments. All the procedures involving rabbits were approved by the Institutional Animal Ethical Committee of the animal center of the Chinese People's Liberation Army (PLA) General Hospital. The rabbits were anaesthetized by injecting pelltobarbitalum natricum (3%, 30 mg kg^{-1}). The neck region was shaved and sterilized, and the right carotid artery was exposed using ophthalmic scissors and tweezers (Figure S6A, Supporting Information). Two hemostatic clamps were applied to occlude the blood flow from the proximal and distal ends of the blood vessel, and a section (about 7 mm) of it in-between the two hemostatic clamps was removed (Figure S6B, Supporting Information). The BC tube with the same dimensions as the resected part of the vessel (Figure S6C, Supporting Information) was prepared and immersed in heparin-NaCl solution (low molecular heparin sodium; Shanghai Fudan Fuhua pharmaceutical Co. Ltd., China) for 10 min before implantation, and heparin-NaCl solution was injected every day for 5 d after implantation to prevent postimplantation thrombosis. The BC tube and rabbit carotid artery were sutured by the end-to-end anastomosis (continuous suture) method. The two ends of tubular BC were sutured with 8-0 Prolene sutures before implantation (Figure S6D, Supporting Information, yellow dashed line). The ends of the blood vessel and BC tube were fixed with 6-8 single knot sutures (8-0 Prolene sutures; Ethicon, USA; Figure S6D, Supporting Information). The blood flew through the BC tube after the removal of the hemostatic clamps (Figure S6E,F, Supporting Information). The implanted blood vessel was sutured, and the wound was closed by suturing the muscles and skin above the blood vessel. The dynamic blood flow of the implanted BC tube was observed by ultrasound imaging in Chinese PLA General Hospital (Philips ultrasound, CX Cart). The images were processed with the Philips DICOM Viewer software.

Supporting Information

Supporting Information is available from the Wiley Online Library or from the author.

Acknowledgements

This work was supported by the National Science Foundation of China (21574050, 21074041, 81361140345, 31470911, 81673039, and 51373043), the "Strategic Priority Research Program" of the Chinese Academy of Sciences (XDA09030305 and XDA09030307), the CAS/SAFEA International Partnership Program for Creative Research Teams. The authors would like to acknowledge Prof. Mario Gauthier (University of Waterloo, Canada) and Dr. Muhammad Wajid Ullah (Huazhong University of Science and Technology) for useful discussions.

Received: November 21, 2016
Revised: February 19, 2017
Published online:

[1] D. Prabhakaran, P. Jeemon, A. Poy, *Circulation* **2016**, *133*, 1605.
[2] C. Tamiello, A. B. C. Buskermolen, F. P. T. Baaijens, J. L. V. Broers, C. V. C. Bouten, *Cell. Mol. Bioeng.* **2016**, *9*, 12.
[3] H. Kurobe, M. W. Maxfield, C. K. Breuer, T. Shinoka, *Stem Cells Transl. Med.* **2012**, *1*, 566.
[4] L. E. Niklason, R. S. Langer, *Transplant Immunol.* **1997**, *5*, 303.
[5] J. H. Lawson, M. H. Glickman, M. Ilzecki, T. Jakimowicz, A. Jaroszynski, E. K. Peden, A. J. Pilgrim, H. L. Prichard, M. Guziewicz, S. Przywara, J. Szmidt, J. Turek, W. Witkiewicz, N. Zapotoczny, T. Zubilewicz, L. E. Niklason, *Lancet* **2016**, *387*, 2026.
[6] F. Yang, R. Murugan, S. Wang, S. Ramakrishna, *Biomaterials* **2005**, *26*, 2603.
[7] S. W. Cho, S. H. Lim, I. K. Kim, Y. S. Hong, S. S. Kim, K. J. Yoo, H. Y. Park, Y. S. Jang, B. C. Chang, C. Y. Choi, K. C. Hwang, B. S. Kim, *Ann. Surg.* **2005**, *241*, 506.
[8] L. Bordenave, P. Menu, C. Baquey, *Expert Rev. Med. Devices* **2008**, *5*, 337.
[9] M. Peck, D. Gebhart, N. Dusserre, T. N. McAllister, N. L'Heureux, *Cells Tissues Organs* **2012**, *195*, 144.
[10] A. Rathore, M. Cleary, Y. Naito, K. Rocco, C. Breuer, *Wiley Interdiscip. Rev.: Nanomed. Nanobiotechnol.* **2012**, *4*, 257.
[11] W. Small IV, P. Singhal, T. S. Wilson, D. J. Maitland, *J. Mater. Chem.* **2010**, *20*, 3356.
[12] Z. Q. Pei, Y. Yang, Q. M. Chen, Y. Wei, Y. Ji, *Adv. Mater.* **2016**, *28*, 156.
[13] C. Chen, J. L. Hu, H. H. Huang, Y. Zhu, T. W. Qin, *Adv. Mater. Technol.* **2016**, *1*, 1600015.
[14] F. El Feninat, G. Laroche, M. Fiset, D. Mantovani, *Adv. Energy Mater.* **2002**, *4*, 91.
[15] Q. Zhao, W. K. Zou, Y. W. Luo, T. Xie, *Sci. Adv.* **2016**, *2*, e1501297.

[16] A. Lendlein, H. Y. Jiang, O. Jünger, R. Langer, *Nature* **2005**, *434*, 879.
[17] A. M. Coppola, L. F. Hu, P. R. Thakre, M. Radovic, I. Karaman, N. R. Sottos, S. White, *Adv. Energy Mater.* **2016**. *18*, 1145.
[18] C. M. Yakacki, R. Shandas, C. Lanning, B. Rech, A. Eckstein, K. Gall, *Biomaterials* **2007**, *28*, 2255.
[19] B. Yuan, Y. Jin, Y. Sun, D. Wang, J. S. Sun, Z. Wang, W. Zhang, X. Y. Jiang, *Adv. Mater.* **2012**, *24*, 890.
[20] Y. Jin, N. X. Wang, B. Yuan, J. S. Sun, M. M. Li, W. F. Zheng, W. Zhang, X. Y. Jiang, *Small* **2013**, *9*, 2410.
[21] P. Y. Gong, W. F. Zheng, Z. Huang, W. Zhang, D. Xiao, X. Y. Jiang, *Adv. Funct. Mater.* **2013**, *23*, 42.
[22] N. X. Wang, L. X. Tang, W. F. Zheng, Y. H. Peng, S. Y. Cheng, Y. F. Lei, L. M. Zhang, B. F. Hu, S. Q. Liu, W. Zhang, X. Y. Jiang, *RSC Adv.* **2016**, *6*, 55054.
[23] W. Czaja, A. Krystynowicz, S. Bielecki, R. M. Brown, *Biomaterials* **2006**, *27*, 145.
[24] R. Jonas, L. F. Farah, *Polym. Degrad. Stab.* **1998**, *59*, 101.
[25] H. Bäckdahl, G. Helenius, A. Bodin, U. Nannmark, B. R. Johansson, B. Risberg, P. Gatenholm, *Biomaterials* **2006**, *27*, 2141.
[26] A. Syensson, E. Nicklasson, T. Harrah, B. Panilaitis, D. L. Kaplan, M. Brittberg, P. Gatenholm, *Biomaterials* **2005**, *26*, 419.
[27] Z. J. Shi, Y. Li, X. L. Chen, H. W. Han, G. Yang, *Nanoscale* **2014**, *6*, 970.
[28] S. H. Li, D. K. Huang, B. Y. Zhang, X. B. Xu, M. K. Wang, G. Yang, Y. Shen, *Adv. Energy Mater.* **2014**, *4*, 1301655.
[29] G. Helenius, H. Bäckdahl, A. Bodin, U. Nannmark, P. Gatenholm, B. Risberg, *J. Biomed. Mater. Res. A* **2006**, *76*, 431.
[30] L. P. Walker, D. B. Wilson, *Bioresour. Technol.* **1991**, *36*, 3.
[31] J. Li, Y. Z. Wan, L. F. Li, H. Liang, J. H. Wang, *Mater. Sci. Eng., C* **2009**, *29*, 1635.
[32] E. Roberts, L. Hardison, R. Brown Jr., *European*, *Patent Number 0186495*, **1986**.
[33] D. Klemm, D. Schumann, U. Udhardt, S. Marsch, *Prog. Polym. Sci.* **2001**, *26*, 1561.
[34] M. Scherner, S. Reutter, D. Klemm, A. Sterner-Kock, M. Guschlbauer, T. Richrer, G. Langebartels, N. Madershahian, T. Wahlers, J. Wippermann, *J. Surg. Res.* **2014**, *189*, 340.
[35] S. S. Zang, R. Zhang, H. Chen, Y. D. Lu, J. H. Zhou, X. Chang, G. X. Qiu, Z. H. Wu, G. Yang, *Mater. Sci. Eng., C* **2015**, *46*, 111.
[36] A. F. Leitão, M. A. Faria, A. M. R. Faustino, R. Moreira, P. Mela, L. Loureiro, I. Silva, M. Gama, *Macromol. Biosci.* **2016**, *16*, 139.
[37] Y. Li, H. Jiang, W. F. Zheng, N. Y. Gong, L. L. Chen, X. Y. Jiang, G. Yang, *J. Mater. Chem. B* **2015**, *3*, 3498.
[38] Y. Li, S. W. Wang, R. Huang, Z. Huang, B. F. Hu, W. F. Zheng, G. Yang, X. Y. Jiang, *Biomacromolecules* **2015**, *16*, 780.
[39] F. Couet, N. Rajan, D. Mantovani, *Macromol. Biosci.* **2007**, *7*, 701.
[40] D. G. White, R. M. Brown Jr., in *Cellulose and Wood-Chemistry and Technology* (Ed: C. Schuerch), John Wiley & Sons Inc., New York **1989**, p. 573.
[41] A. H. Slyper, *J. Clin. Endocrinol. Metab.* **2004**, *89*, 3089.
[42] M. J. Kim, J. H. Kim, G. J. Yi, S. H. Lim, Y. S. Hong, D. J. Chung, *Macromol. Res.* **2008**, *16*, 345.
[43] R. Gauvin, T. Ahsan, D. Larouche, P. Lévesque, J. Dubé, F. A. Auger, R. M. Nerem, L. German, *Tissue Eng., Part A* **2010**, *16*, 1737.
[44] N. Chiaoprakobkij, N. Sanchavanakit, K. Subbalekha, P. Pavasant, M. Phisalaphong, *Carbohydr. Polym.* **2011**, *85*, 548.